15-Epi-LXA$_4$ and 17-epi-RvD1 restore TLR9-mediated impaired neutrophil phagocytosis and accelerate resolution of lung inflammation

Meriem Sekheri[a,b], Driss El Kebir[b], Natalie Edner[b], and János G. Filep[a,b,1]

[a]Department of Pathology and Cell Biology, University of Montreal, Montreal, QC H3T 1J4, Canada; and [b]Research Centre, Maisonneuve-Rosemont Hospital, Montreal, QC H1T 2M4, Canada

Edited by Charles N. Serhan, Brigham and Women's Hospital, Harvard Medical School, Boston, MA, and accepted by Editorial Board Member Carl F. Nathan February 25, 2020 (received for review November 15, 2019)

Timely resolution of bacterial infections critically depends on phagocytosis of invading pathogens by polymorphonuclear neutrophil granulocytes (PMNs), followed by PMN apoptosis and efferocytosis. Here we report that bacterial DNA (CpG DNA) and mitochondrial DNA impair phagocytosis and attenuate phagocytosis-induced apoptosis in human PMNs through Toll-like receptor 9 (TLR9)-mediated release of neutrophil elastase and proteinase 3 and subsequent down-regulation of the complement receptor C5aR. Consistently, CpG DNA delays pulmonary clearance of *Escherichia coli* in mice and suppresses PMN apoptosis, efferocytosis, and generation of proresolving lipid mediators, thereby prolonging lung inflammation evoked by *E. coli*. Genetic deletion of TLR9 renders mice unresponsive to CpG DNA. We also show that aspirin-triggered 15-epi-lipoxin A$_4$ (15-epi-LXA$_4$) and 17-epi-resolvin D1 (17-epi-RvD1) through the receptor ALX/FPR2 antagonize cues from CpG DNA, preserve C5aR expression, restore impaired phagocytosis, and redirect human PMNs to apoptosis. Treatment of mice with 15-epi-LXA$_4$ or 17-epi-RvD1 at the peak of inflammation accelerates clearance of bacteria, blunts PMN accumulation, and promotes PMN apoptosis and efferocytosis, thereby facilitating resolution of *E. coli*-evoked lung injury. Collectively, these results uncover a TLR9-mediated endogenous mechanism that impairs PMN phagocytosis and prolongs inflammation, and demonstrate both endogenous and therapeutic potential for 15-epi-LXA$_4$ and 17-epi-RvD1 to restore impaired bacterial clearance and facilitate resolution of acute lung inflammation.

resolution of inflammation | phagocytosis | neutrophils | TLR9 | aspirin-triggered LXA$_4$ and RvD1

Timely resolution of bacterial infection critically depends on clearance of invading pathogens by polymorphonuclear neutrophil granulocytes (PMNs) followed by PMN apoptosis and efferocytosis (1–3). Impaired bacterial clearance and delayed PMN apoptosis underlie numerous pathologies, including sepsis (4) and PMN-mediated airway diseases (5, 6). PMN-derived proteases are required for antimicrobial defense (7) but are also capable of inducing PMN dysfunction and inflicting tissue damage (8, 9). Neutrophil elastase (NE) plays a pivotal role in airway remodeling (10) and modulates the local inflammatory response through proteolysis of cytokines, chemokines, or their receptors, including CXCR1 (11) and the complement receptors CR1 (CD11b/CD18) (12) and C5aR (CD88) (13). Diminished expression of CXCR1 or CD11b/CD18 on PMNs is associated with reduced phagocytosis of *Pseudomonas aeruginosa* (11, 12). The PMN chemoattractant C5a through C5aR enhances phagocytosis and intracellular killing of C3b-opsonized bacteria (14, 15). Consistently, blocking of C5aR was shown to inhibit phagocytosis of *Escherichia coli* by human PMNs (14), and genetic deletion of C5aR impaired clearance of *P. aeruginosa* and enhanced mortality in mice (16).

In the inflammatory microenvironment, PMNs respond to cues from both pathogen-associated and danger-associated molecular patterns. Among these signals are bacterial DNA (CpG DNA) released from proliferating or dying bacteria and mitochondrial DNA (mtDNA) released from injured cells. Both CpG DNA and mtDNA are rich in unmethylated CpG dinucleotides (17, 18) and may contribute to ongoing inflammation. CpG DNA has been detected in the blood of critically ill patients (19) and in their airways (20). CpG DNA promotes PMN trafficking to primary sites of infection (20–22), induces interleukin-8 (IL-8) production (23, 24), and delays neutrophil apoptosis (25, 26). Mitochondrial DNA is present in the blood of critically ill patients (27, 28) and triggers an immune response through activation of the inflammasome (18, 29). However, it is not known whether CpG DNA or mtDNA regulates phagocytosis and phagocytosis-induced PMN apoptosis, a critical step in the resolution of inflammation.

Resolution of inflammation is an active process governed by specialized proresolving lipid and protein mediators (2, 30–33). Among the lipid mediators are lipoxin A$_4$ (LXA$_4$), 15-epi-LXA$_4$, and 17-epi-resolvin D1 (17-epi-RvD1), typically generated by transcellular biosynthesis at sites of inflammation (31, 34). Lipoxins and resolvins inhibit PMN trafficking into inflamed tissues and facilitate recruitment of monocytes/macrophages,

Significance

Timely resolution of bacterial infections critically depends on phagocytosis of invading pathogens by polymorphonuclear neutrophil granulocytes, followed by neutrophil apoptosis and removal by macrophages. Neutrophils integrate cues from the inflammatory microenvironment. Here we show a Toll-like receptor 9-mediated mechanism, involving regulation of phagocytosis and phagocytosis-induced neutrophil apoptosis, by which bacterial DNA, a pathogen-associated molecular pattern, and the danger signal mitochondrial DNA may impair host defense to bacteria and prolong the inflammatory response. We also report that the proresolution aspirin-triggered lipids 15-epi-lipoxin A$_4$ and 17-epi-resolvin D1 restore impaired phagocytosis and enhance bacterial clearance and phagocytosis-induced neutrophil apoptosis, thereby facilitating resolution of acute lung inflammation. These findings imply the lipoxin receptor ALX/FPR2 as a potential therapeutic target for combating bacterial infections.

Author contributions: M.S., D.E.K., and J.G.F. designed research; M.S., D.E.K., N.E., and J.G.F. performed research; M.S., D.E.K., N.E., and J.G.F. analyzed data; and J.G.F. wrote the paper.

The authors declare no competing interest.

This article is a PNAS Direct Submission. C.N.S. is a guest editor invited by the Editorial Board.

This open access article is distributed under Creative Commons Attribution-NonCommercial-NoDerivatives License 4.0 (CC BY-NC-ND).

See online for related content such as Commentaries.

[1]To whom correspondence may be addressed. Email: janos.g.filep@umontreal.ca.

This article contains supporting information online at https://www.pnas.org/lookup/suppl/doi:10.1073/pnas.1920193117/-/DCSupplemental.

First published March 23, 2020.

efferocytosis, and tissue regeneration (reviewed in refs. 31 and 32). Self-limiting infection in mice is biased toward a proresolving lipid profile, including generation of LXA_4 and resolvin D5 (5, 32, 35), concurrent with lower antibiotic requirements (35).

Here, we report that CpG DNA and mtDNA impair phagocytosis through Toll-like receptor 9 (TLR9)-mediated release of NE and proteinase 3 (PR3) and subsequent down-regulation of C5aR, thereby reducing phagocytosis-induced apoptosis in human PMNs. By activating the receptor ALX/FPR2, 15-epi-LXA_4 and 17-epi-RvD1 counterregulate signals from CpG DNA, restore phagocytosis, and redirect PMNs to apoptosis. In mice, CpG DNA delays pulmonary clearance of *E. coli*, suppresses PMN apoptosis and efferocytosis, and prolongs *E. coli*-evoked lung inflammation. Treatment with 15-epi-LXA_4 or 17-epi-RvD1 enhances bacterial clearance and PMN apoptosis, thereby promoting resolution of inflammation. These results shed light on how CpG DNA and mtDNA contribute to PMN dysfunction and ongoing inflammation. Our results also identify an effector mechanism, restoring C5aR-mediated phagocytosis-induced PMN apoptosis, by which 15-epi-LXA_4 and 17-epi-RvD1 facilitate timely resolution of infections.

Results

CpG DNA Impairs Phagocytosis-Induced Apoptosis in Human Neutrophils. Earlier studies showed that CpG DNA delays constitutive apoptosis in human PMNs (25, 26). We used opsonized *E. coli* and yeast as target pathogens to assess the impact of CpG DNA on phagocytosis-induced PMN apoptosis. CpG DNA reduced phagocytosis of fluorescein isothiocyanate (FITC)-labeled *E. coli* by isolated PMNs (Fig. 1*A*) as well as by PMNs and monocytes in whole blood (Fig. 1*B*). Consistent with published data (36, 37), phagocytosis of opsonized yeast evoked apoptosis as assessed at 4 and 24 h of culture (Fig. 1 *C* and *D*) and increased caspase-8 and caspase-3 activity (Fig. 1 *E* and *F*). Culture of PMNs with CpG DNA markedly attenuated phagocytosis-induced apoptosis (Fig. 1 *C* and *D*) and suppressed activation of caspase-8 and caspase-3 (Fig. 1 *E* and *F*).

Because efficient phagocytosis and intracellular killing of pathogens depend on functions of both C3bR and C5aR (12, 14, 15), we investigated the impact of CpG DNA on these receptors. Confirming published data (25, 26), CpG DNA evoked concentration-dependent increases in CD11b expression (Fig. 2 *A* and *B*). By contrast, using a monoclonal antibody (mAb) specific for the N terminus of C5aR, we detected significant reductions in cell-surface C5aR expression (Fig. 2 *A* and *B*), indicating receptor cleavage.

We used a phosphokinase array to investigate the signaling pathways activated by CpG DNA in human PMNs. A clear difference in phosphorylation of the Src kinase Hck, but not Lyn or Fgr, in response to CpG DNA was detected (Fig. 2*C*), which mediates release of contents from primary (azurophil) granules. We detected increased NE (Fig. 2*D*) and PR3 (Fig. 2*E*) in the culture media of human PMNs challenged with CpG DNA. To investigate if reduced cell-surface C5aR expression was due to enzymatic cleavage in response to CpG DNA, neutrophils were assessed for C5aR expression in the presence of various protease inhibitors. Down-regulation of C5aR expression by CpG DNA was partially prevented by neutrophil elastase inhibitor IV (NEI) and a neutralizing anti-PR3 Ab. We calculated 60 ± 5% and 32 ± 5% (n = 5) inhibition of CpG DNA-evoked changes, respectively. Phenylmethanesulfonylfluoride (PMSF) also attenuated CpG DNA-evoked decreases in C5aR expression, whereas a cathepsin G inhibitor and 1,10-phenantroline were without detectable effects (Fig. 2*F*). Consistently, NEI, but not cathepsin G inhibitor, partially reversed CpG DNA reductions in phagocytosis of FITC-labeled *E. coli* (Fig. 2*G*). Culture of PMNs with purified human NE or PR3 at concentrations comparable to those detected in the supernatants of CpG DNA challenged

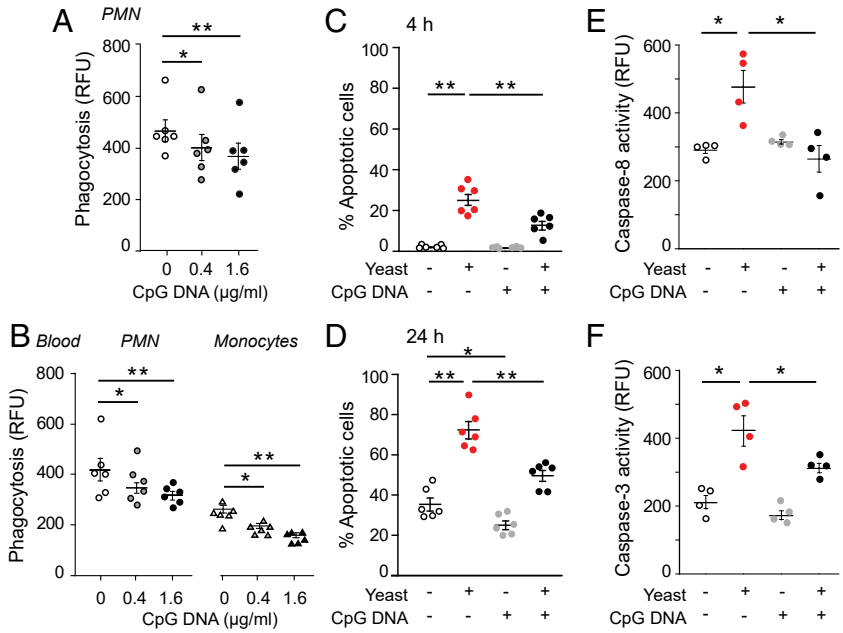

Fig. 1. CpG DNA impairs phagocytosis-induced neutrophil apoptosis. (*A* and *B*) Human PMNs (5×10^6 cells per milliliter) (*A*) or whole blood (*B*) was cultured with CpG DNA for 60 min and then mixed with opsonized FITC-labeled *E. coli* at a ratio of 1:7 for 30 min. Extracellular fluorescence was quenched with 0.2% trypan blue and intracellular fluorescence was analyzed with flow cytometry. Results are means ± SEM (n = 6 different blood donors). *$P < 0.05$, **$P < 0.01$. (*C* and *D*) PMNs were cultured for 4 h (*C*) or 24 h (*D*) with yeast at a ratio of 1:5 and stained with acridine orange (10 μg/mL), and apoptosis was assessed by nuclear morphology (condensed or fragmented chromatin) under a fluorescence microscope. Results are means ± SEM (n = 6 different blood donors). *$P <$ 0.05, **$P < 0.01$. (*E* and *F*) Caspase-8 (*E*) and caspase-3 (*F*) activity was assessed at 4 h of culture with flow cytometry using FITC-labeled Z-Ile-Glu(OMe)-Thr-Asp(OMe)-fluoromethyl ketone and Z-Asp(OMe)-Glu(OMe)-Val-Asp(OMe)-fluoromethyl ketone, respectively. Results are means ± SEM (n = 4 different blood donors). *$P < 0.05$ (Dunn's multiple contrast hypothesis test). RFU, relative fluorescence unit.

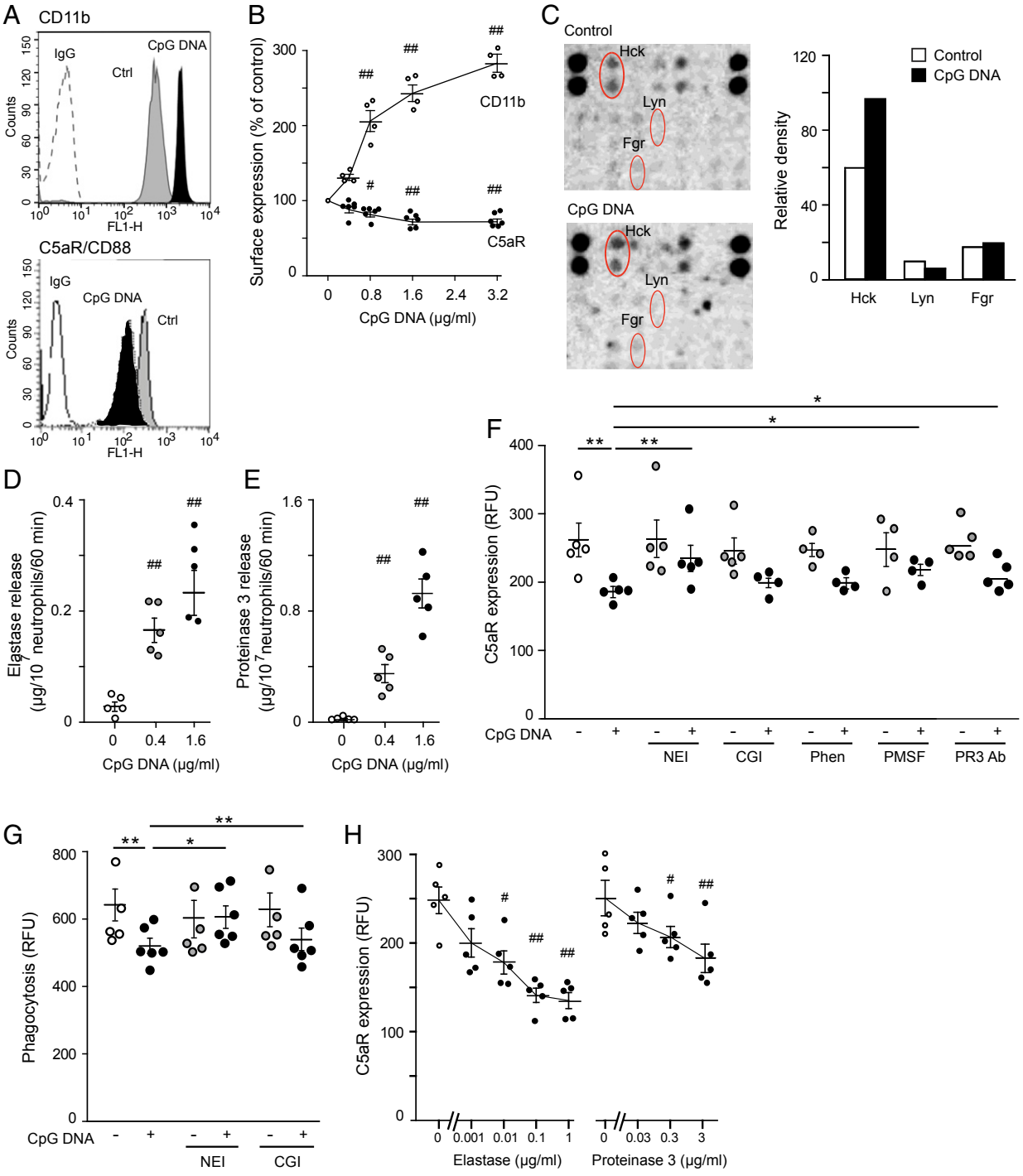

Fig. 2. CpG DNA inactivates C5aR through inducing NE and PR3 release in human neutrophils. (*A* and *B*) PMNs (5×10^6 cells per milliliter) were cultured with CpG DNA for 60 min. Cell-surface expression of CD11b and C5aR (CD88) was analyzed by flow cytometry using anti-CD11b mAb (clone D12) and anti-CD88 mAb (clone S5/1), respectively. Representative histograms (*A*) and concentration-dependent actions of CpG DNA after correction with staining with appropriate isotype-matched irrelevant antibodies (IgG) (*B*). Results are means ± SEM ($n = 4$ or 5 different blood donors). $^{\#}P < 0.05$, $^{\#\#}P < 0.01$ vs. vehicle (0 μg/mL) (Wilcoxon–Wilcox test). (*C*) Proteome profiler array on human PMNs challenged with CpG DNA (1.6 μg/mL) or vehicle (control) for 30 min and densitometry analysis of Src kinases. Blots and densitometry data are representative of three independent arrays with different blood donors. (*D* and *E*) NE (*D*) and PR3 levels (*E*) in the culture medium were measured at 1 h post CpG DNA by colorimetric assays using specific substrates. Results are means ± SEM ($n = 5$ independent experiments). $^{\#\#}P < 0.01$ vs. vehicle (0 μg/mL) (Wilcoxon–Wilcox test). (*F*) Surface C5aR expression. Human PMNs were incubated with neutrophil elastase inhibitor IV (20 μM), cathepsin G inhibitor (CGI; 20 μM), 1,10-phenantroline (Phen; 4 mM), PMSF (2 mM), or neutralizing anti-PR3 Ab (5 μg/mL) for 30 min and then challenged with CpG DNA (1.6 μg/mL) for 60 min. Surface expression of C5aR was analyzed by flow cytometry. Results are means ± SEM ($n = 4$ or 5 different blood donors). $^{*}P < 0.05$, $^{**}P < 0.01$ (Dunn's multiple contrast hypothesis test). (*G*) NEI restores phagocytosis. PMNs were preincubated with NEI or CGI for 30 min and challenged with CpG DNA (1.6 μg/mL) in the presence of opsonized FITC-labeled *E. coli* at a ratio of 1:7 for 30 min. Extracellular fluorescence was quenched with 0.2% trypan blue and intracellular fluorescence was analyzed with flow cytometry. Results are means ± SEM ($n = 5$ or 6 different blood donors). $^{*}P < 0.05$, $^{**}P < 0.01$ (Dunn's multiple contrast hypothesis test). (*H*) NE and PR3 down-regulate C5aR expression. PMNs were challenged with purified human NE or PR3 for 60 min. Results are means ± SEM ($n = 5$ different blood donors). $^{\#}P < 0.05$, $^{\#\#}P < 0.01$ vs. control (0 μg/mL) (Wilcoxon–Wilcox test).

PMNs and reduced surface expression of C5aR (Fig. 2*H*). These findings indicate that both NE and PR3 have the ability to cleave C5aR and suggest that NE is dominant over PR3 for impairing phagocytosis-induced apoptosis in response to CpG DNA. Culture of PMNs with either CpG DNA or *E. coli* also resulted in decreased surface expression of ALX/FPR2; however, the effects of CpG DNA and *E. coli* were not additive (*SI Appendix*, Fig. S1).

Treatment with a TLR9 inhibitory oligodeoxynucleotide (ODN) (38) almost completely prevented CpG DNA suppression of phagocytosis-induced PMN apoptosis, whereas the control ODN was without effects (*SI Appendix*, Fig. S2), confirming the involvement of TLR9 in mediating these actions of CpG DNA on human PMNs.

Because of similarities in the structure of CpG DNA and mtDNA, we studied whether mtDNA could mimic the actions of CpG DNA. Like CpG DNA (25, 26), mtDNA also delayed constitutive PMN apoptosis in a concentration-dependent manner (*SI Appendix*, Fig. S3*A*). Furthermore, mtDNA impaired phagocytosis-induced apoptosis in PMNs in parallel with reductions in caspase-8 and caspase-3 activity (*SI Appendix*, Fig. S3 *B–E*) and evoked release of neutrophil elastase (*SI Appendix*, Fig. S3*F*).

CpG DNA Impairs Bacterial Clearance and Resolution of *E. coli* Pneumonia. Having shown that CpG DNA attenuated phagocytosis-induced apoptosis in vitro, we investigated the impact of CpG DNA on bacterial clearance and the resolution of PMN-mediated inflammation in mice. We used a model of lung inflammation induced by intratracheal instillation of live *E. coli*, which resolves within 48 h without treatment. As anticipated, *E. coli* evoked lung injury that peaked at around 6 h post injection and resolved by 48 h (Fig. 3). Wild-type (WT) mice rapidly cleared *E. coli* (Fig. 3*A*) in parallel with dissipation of inflammatory infiltrates in the lung (Fig. 3 *B* and *C*). The lungs appeared to be almost normal by 48 h. This is reflected by reductions in *E. coli*-induced edema (Fig. 3*D* and *SI Appendix*, Fig. S4*A*), bronchoalveolar lavage (BAL) fluid leukocytes (*SI Appendix*, Fig. S4*B*), and PMNs (Fig. 3*E*) and increases in BAL fluid monocytes/macrophages (Fig. 3*F*), the number of apoptotic PMNs (Fig. 3*G*), and efferocytosis (Fig. 3*H*). *E. coli* infection was also associated with marked increases in lavage fluid levels of 15-epi-LXA_4 and RvD1 at 6 h post injection (Fig. 3 *I* and *J*), indicating activation of the resolution mechanism. Elevations in 15-epi-LXA_4 and RvD1 levels persisted at 24 h post injection, returning to baseline levels at 48 h. Intraperitoneal (i.p.) injection of CpG DNA alone produced no detectable inflammation in the lung, whereas it delayed bacterial clearance (Fig. 3*A*) and prolonged pulmonary inflammation (Fig. 3*B*). Thus, lung inflammatory infiltration (Fig. 3 *B* and *C*), edema (Fig. 3*D* and *SI Appendix*, Fig. S4*A*), and neutrophil accumulation (Fig. 3 *C* and *E*) persisted for at least 48 h in mice that received *E. coli* plus CpG DNA. The percentage of apoptotic PMNs was markedly lower in mice simultaneously injected with *E. coli* and CpG DNA at 24 h, followed by increases at 48 h (Fig. 3*G*), indicating that CpG DNA delayed, but did not inhibit, PMN apoptosis. However, the percentage of macrophages containing apoptotic bodies remained low even at 48 h post injection (Fig. 3*H*). Furthermore, no significant increases in lavage fluid levels of 15-epi-LXA_4 and RvD1 were detectable during the entire observation period (Fig. 3 *I* and *J*).

Like WT mice, *Tlr9*$^{-/-}$ mice rapidly cleared intratracheally instilled *E. coli* and resolved pulmonary inflammation (*SI Appendix*, Fig. S5). Coadministration of CpG DNA with *E. coli*, however, did not delay *E. coli* clearance and did not promote edema formation or tissue PMN accumulation (*SI Appendix*, Fig. S5). These would indicate that the actions of CpG DNA in mice were also mediated through TLR9.

15-Epi-LXA_4 and 17-Epi-RvD1 Restore Phagocytosis-Induced Apoptosis in Human PMNs. Because 15-epi-LXA_4 and 17-epi-RvD1 down-regulate CD11b expression (31, 32) and enhance efferocytosis (39, 40), we studied their actions on phagocytosis-induced apoptosis and cellular signaling. While 15 epi-LXA_4 alone did not affect CD11b or C5aR expression or induce elastase release, it attenuated CpG DNA-evoked up-regulation of CD11b expression and partially prevented down-regulation of C5aR expression with an apparent maximum action at 1 μM (Fig. 4 *A* and *B*). 15-Epi-LXA_4 markedly reduced NE release (Fig. 4*C*) without directly affecting the activity of purified NE (Fig. 4*D*). Consistently, 15-epi-LXA_4 efficiently countered CpG DNA-evoked decreases in phagocytosis of opsonized FITC-labeled *E. coli* by isolated PMNs (Fig. 4*E*) as well as by blood PMNs and monocytes (*SI Appendix*, Fig. S6), and augmented phagocytosis-induced apoptosis (Fig. 4*F*) concomitant with increases in caspase-8 and caspase-3 activity (Fig. 4 *G* and *H*). The 15-epi-LXA_4 actions were prevented by the NADPH oxidase inhibitor diphenyleneiodonium (DPI) (Fig. 4*F*). Similar to 15-epi-LXA_4, 17-epi-RvD1 markedly attenuated CpG DNA-evoked changes in CD11b and C5aR expression and NE release (*SI Appendix*, Fig. S7 *A–C*), restored phagocytosis (*SI Appendix*, Fig. S7*D*), and augmented phagocytosis-induced PMN apoptosis (*SI Appendix*, Fig. S7 *E–G*). On a molar basis, 4 to 5 times less 17-epi-RvD1 was required to produce inhibition similar to that of 15-epi-LXA_4. As anticipated, these actions of 15-epi-LXA_4 and 17-epi-RvD1 were effectively blocked by the ALX/FPR2 antagonists Boc-2 and WRW4 (*SI Appendix*, Fig. S8).

15-Epi-LXA_4 and 17-Epi-RvD1 Restore Impaired Bacterial Clearance by CpG DNA and Enhance Resolution of *E. coli* Pneumonia. Having shown the ability of 15-epi-LXA_4 and 17-epi-RvD1 to restore impaired phagocytosis and phagocytosis-induced apoptosis in human PMNs, next we investigated whether these lipids could accelerate the resolution of *E. coli* plus CpG DNA-induced lung inflammation in mice. Treatment of mice with a bolus injection of either 15-epi-LXA_4 or 17-epi-RvD1 at 6 h post *E. coli* plus CpG DNA, near the peak of inflammation (Fig. 5*A*), accelerated clearance of bacteria (Fig. 5*B*). Thus, no apparent bacteria were detectable in the lung at 48 h. Antiinflammatory and proresolving actions of 15-epi-LXA_4 and 17-epi-RvD1 were also evident as both lipids markedly reduced inflammatory infiltrate and injury at 24 h, and the lung appeared almost normal at 48 h (Fig. 5 *C* and *D*). Both 15-epi-LXA_4 and 17-epi-RvD1 reduced edema formation (Fig. 5 *E* and *F*). We also observed over a period of 48 h of administering 15 epi-LXA_4 or 17-epi-RvD1 decreases in BAL fluid total leukocyte (Fig. 5*G*) and PMN numbers (Fig. 5*H*), with increases in the number of monocytes/macrophages at 24 h (Fig. 5*I*). Decreases in BAL fluid PMN count occurred in parallel with increases in the percentage of annexin V-positive PMNs (Fig. 5*J*) and the percentage of macrophages containing apoptotic bodies (Fig. 5*K*). 15-Epi-LXA_4 also reduced BAL fluid levels of IL-6, tumor necrosis factor α (TNF-α), and G-CSF at 24 and 48 h without affecting the time course of changes in IL-1β or KC (*SI Appendix*, Fig. S9). *E. coli* plus CpG DNA-evoked increases in IL-10 levels apparently peaked at 6 h post injection followed by rapid declines at 24 and 48 h, which was prevented by 15 epi-LXA_4 at 48 h post *E. coli* plus CpG DNA (*SI Appendix*, Fig. S9).

Discussion

Our results uncovered an unexpected action for CpG DNA and mtDNA to influence phagocytosis and the fate of PMNs, and consequently the duration of inflammation. By inducing NE and PR3 release and cleavage of C5aR, CpG DNA and mtDNA impaired phagocytosis and phagocytosis-induced PMN apoptosis, thereby delaying the resolution of inflammation. We also show that by preventing down-regulation of C5aR expression, aspirin-triggered 15-epi-LXA_4 and 17-epi-RvD1 can restore impaired phagocytosis and bacterial clearance and facilitate resolution of *E. coli*-evoked PMN-dependent pulmonary inflammation in vivo.

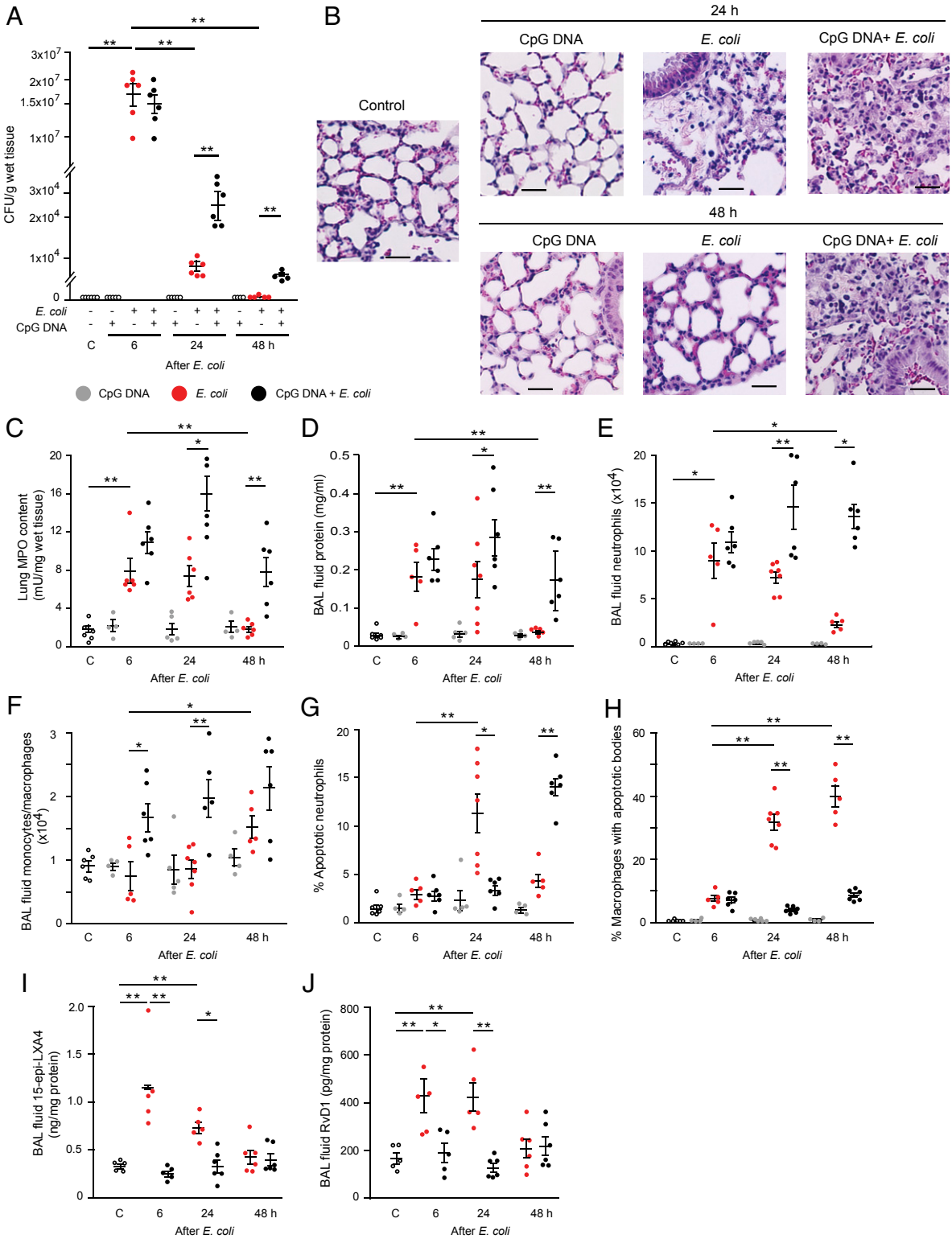

Fig. 3. CpG DNA impairs bacterial clearance and delays resolution of *E. coli* pneumonia in mice. Female C57BL/6 mice were injected intratracheally with 5×10^6 live *E. coli* with or without CpG DNA (1 μg/g b.w., i.p.). (*A* and *C*) At 6, 24, or 48 h, the lungs were removed without lavage and analyzed for *E. coli* content (*A*) and tissue myeloperoxidase (MPO) activity (*C*). (*B*) Lung tissue sections from naïve mice (control) and mice challenged with *E. coli* and CpG DNA were stained with hematoxylin and eosin. (Scale bars, 100 μm.) (*D*–*J*) In separate groups of mice, bronchoalveolar lavage fluid protein concentration (*D*), neutrophil (*E*) and monocyte/macrophage numbers (*F*), percentage of annexin V-positive (apoptotic) neutrophils (*G*), percentage of macrophages containing apoptotic bodies (*H*), and lavage fluid levels of 15-epi-LXA_4 (*I*) and RvD1 (*J*) were determined. Results are means ± SEM ($n = 5$ to 7 mice per group). $^*P < 0.05$, $^{**}P < 0.01$ (Dunn's multiple contrast hypothesis test).

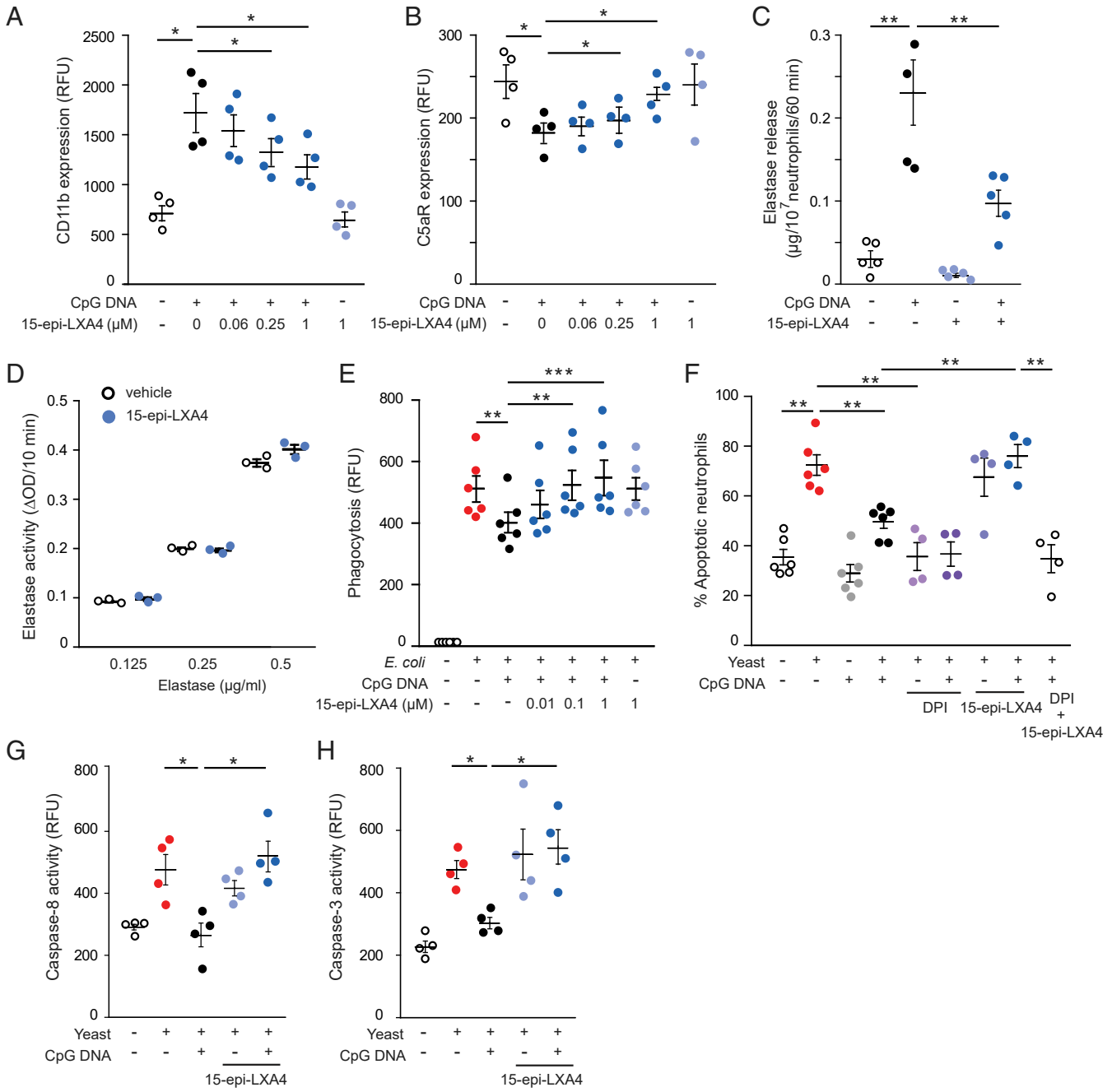

Fig. 4. 15-Epi-LXA$_4$ restores impaired phagocytosis-induced neutrophil apoptosis. (*A–C*) Human PMNs (5×10^6 cells per milliliter) were cultured for 10 min with 15-epi-LXA$_4$ and then with CpG DNA (1.6 μg/mL) for 60 min. Surface expression of CD11b (*A*) and C5aR (CD88) (*B*) was assessed by flow cytometry; neutrophil elastase release was measured with a colorimetric assay using *N*-methoxysuccinyl-Ala-Ala-Pro-Val-*p*-nitroanilide as a substrate (*C*). Results are means ± SEM ($n = 4$ or 5 different blood donors). *$P < 0.05$, **$P < 0.01$. (*D*) Purified human neutrophil elastase was incubated with 15-epi-LXA$_4$ for 10 min and then elastase activity was monitored. Results are means ± SEM ($n = 3$ independent experiments). (*E*) PMNs were cultured with 15-epi-LXA$_4$ for 10 min and CpG DNA for 60 min and then with opsonized FITC-labeled *E. coli* (7 bacteria per neutrophil) for 30 min. Extracellular fluorescence was quenched with 0.2% trypan blue and intracellular fluorescence was analyzed with flow cytometry. Results are means ± SEM ($n = 6$ different blood donors). **$P < 0.01$, ***$P < 0.001$. (*F–H*) Neutrophils were cultured with 15-epi-LXA$_4$ or DPI (20 μM) for 10 min, followed by CpG DNA for 60 min and then with yeast (5 yeast particles per cell). (*F*) Apoptosis was assessed by nuclear morphology at 24 h of culture following staining with acridine orange (10 μg/mL). Results are means ± SEM ($n = 4$ to 6 different blood donors). (*G* and *H*) Caspase-8 (*G*) and caspase-3 (*H*) activity was assessed at 4 h of culture with flow cytometry using FITC-labeled Z-Ile-Glu(OMe)-Thr-Asp(OMe)-fluoromethyl ketone and Z-Asp(OMe)-Glu(OMe)-Val-Asp(OMe)-fluoromethyl ketone, respectively. Results are means ± SEM ($n = 4$ different blood donors). *$P < 0.05$, **$P < 0.01$ (Dunn's multiple contrast hypothesis test).

Typically, phagocytosis of bacteria accelerates PMN apoptosis and promotes their removal from inflamed tissues via efferocytosis, ultimately leading to the resolution of inflammation. Ligation of CD11b following PMN adhesion to the endothelium and phagocytosis of complement-opsonized microbes generates survival cues for PMNs, which are overridden by phagocytosis-triggered reactive oxygen species (ROS)-mediated activation of caspase-8 and caspase-3, redirecting PMNs to apoptosis (36, 37). These led us to investigate the impact of CpG DNA on PMN phagocytosis and the resolution of infection.

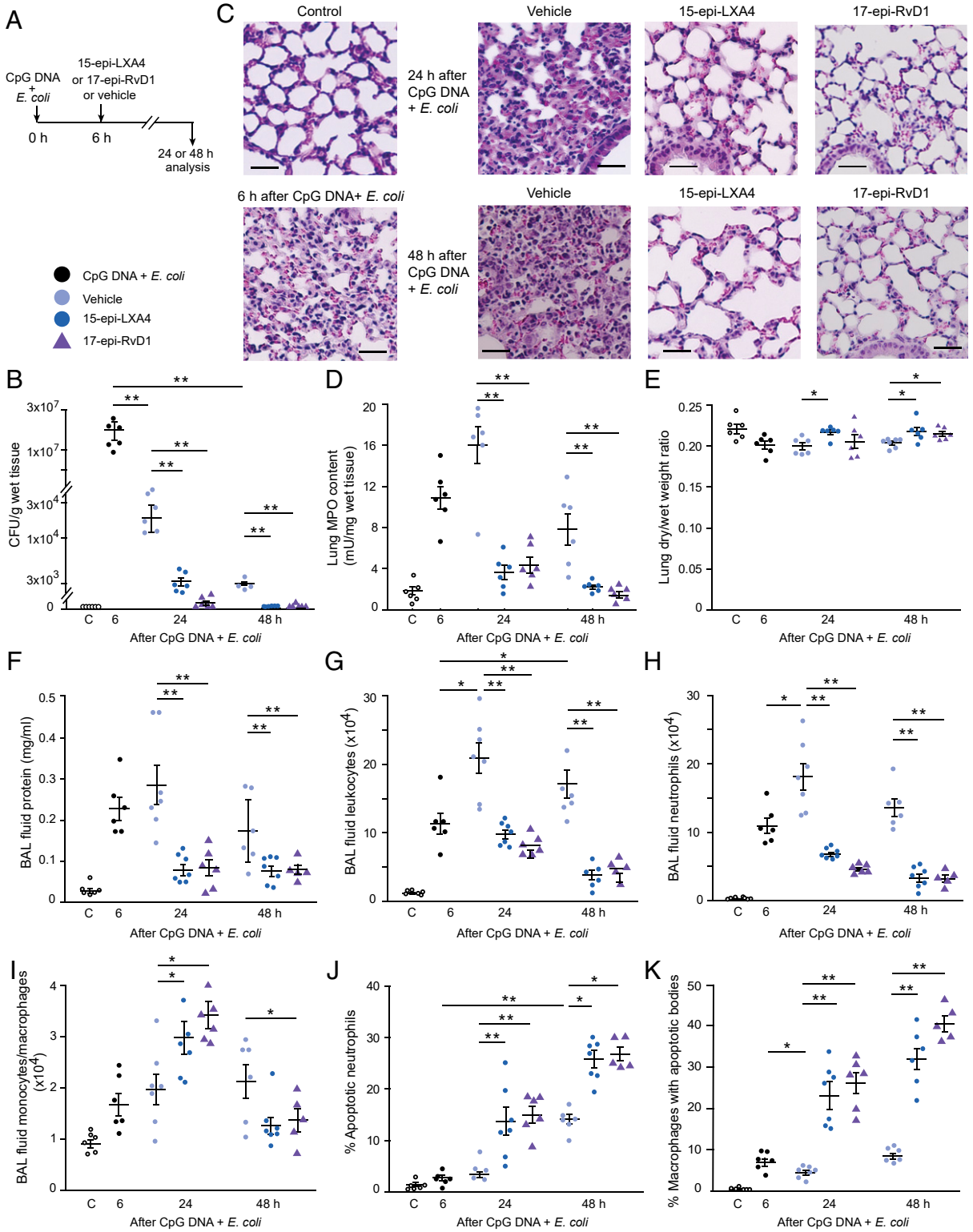

Fig. 5. 15-Epi-LXA$_4$ and 17-epi-RvD1 facilitate bacterial clearance and enhance resolution of lung inflammation. (*A*) Female C57BL/6 mice were treated with 15-epi-LXA$_4$ (125 ng/g b.w., i.p.), 17-epi-RvD1 (25 ng/g b.w., i.p.), or vehicle 6 h after intratracheal instillation of 5×10^6 live *E. coli* plus CpG DNA (1 μg/g b.w., i.p.). Mice were killed at the indicated times, and the lungs were processed for analysis without lavage or bronchoalveolar lavage was performed. (*B*) *E. coli* content. (*C*) Lung tissue sections from naïve mice (control) and mice challenged with *E. coli* + CpG DNA and treated with 15-epi-LXA$_4$, 17-epi-RvD1, or vehicle. Hematoxylin and eosin stain. (Scale bars, 100 μm.) (*D*) Lung tissue MPO content. (*E*) Lung dry-to-wet weight ratio. (*F–K*) Bronchoalveolar lavage fluid protein concentration (*F*), total leukocyte (*G*), neutrophil (*H*), and monocyte/macrophage counts (*I*), percentage of annexin V-positive (apoptotic) neutrophils (gated as Ly6G$^+$ cells) (*J*), and percentage of macrophages containing apoptotic bodies (*K*) were determined. Results are means ± SEM (n = 6 or 7 mice per group). *$P < 0.05$, **$P < 0.01$ (Dunn's multiple contrast hypothesis test).

Down-regulation of C5aR by C5a, PMA, and bacterial fMLF has previously been linked to reduced PMN chemotaxis and phagocytosis (16, 41). Enzymatic degradation by NE or cathepsin G (13), shedding (41), and intracellular degradation following C5a-induced internalization (13) have been implied as potential mechanisms responsible for loss of C5aR. We found that C5aR expressed on PMNs is sensitive to enzymatic degradation in response to CpG DNA and mtDNA, and this leads to PMN dysfunction. CpG DNA and mtDNA evoked release of NE and PR3 from human PMNs at amounts comparable to those of purified NE or PR3 sufficient to induce C5aR cleavage. Furthermore, loss of C5aR by CpG DNA was largely prevented by an NE inhibitor and to a lesser degree by PR3 blockade, but not a cathepsin G inhibitor, pointing toward NE as a predominant serine protease responsible for this action. Consistently, pharmacological inhibition of NE reversed CpG DNA suppression of *E. coli* phagocytosis in vitro. Intriguingly, CpG DNA reduction of phagocytosis and phagocytosis-induced PMN apoptosis occurred despite up-regulation of CD11b, indicating that a delicate balance between CD11b and C5aR, rather than CD11b expression per se, governs complement-mediated phagocytosis. The mechanism by which C5aR affects lateral clustering of integrin receptors, which initiates phagocytosis (42), remains to be investigated. The importance of C5aR is further underlined by the elaborate strategies evolved by bacteria to avoid the complement system, including inhibition of C5a generation or blockade of C5aR (43).

Consistent with the results obtained in human PMNs, mice that received CpG DNA were less efficient in clearing *E. coli* than vehicle-treated controls in parallel with prolongation of the inflammatory response. In particular, CpG DNA markedly delayed the rapid fall in tissue and BAL fluid PMNs and development of PMN apoptosis, efferocytosis, and proresolving lipid profile, which occur during spontaneous resolution of *E. coli* pneumonia. Our in vitro results point to inhibition by CpG DNA or mtDNA of phagocytosis-induced PMN apoptosis, although we cannot exclude the possibility that other mechanisms may have contributed to delayed PMN apoptosis and persisting inflammation in vivo.

Multiple cytosolic DNA sensors have been identified over the past years (44). We found that blockade of TLR9 with an inhibitory ODN in human PMNs or genetic deletion of TLR9 in mice rendered them unresponsive to CpG DNA. This telomere-derived suppressive ODN disrupts interaction of CpG DNA with TLR9 in endosomal vesicles without affecting cellular CpG DNA uptake (38). Ligation of TLR9 through recruitment of preferential TIR domain-containing adaptor proteins triggers downstream signaling pathways to orchestrate distinct cellular responses (45, 46). Recruitment of MyD88 and TRAF6 leads to activation of nuclear factor κB (NF-κB) and induction of proinflammatory gene expression (46). This mechanism likely contributes to massive production of TNF-α and IL-6 in mice in response to *E. coli* plus CpG DNA. CpG DNA induces NF-κB–mediated transcription of inducible nitric oxide synthase (iNOS) in human PMNs (24), which, in turn, could activate the *src* family of nonreceptor tyrosine kinases (47). CpG DNA was found to activate Hck in murine macrophages (47, 48). We detected increased phosphorylation of Hck, but not Fgr or Lyn, in response to CpG DNA in human PMNs. These kinases control release of contents from distinct granule populations and Hck translocates to the primary granules following cell activation (9). Thus, our results would link CpG DNA-induced Hck phosphorylation to release of NE and PR3, though the precise mechanism requires further investigations.

15-Epi-LXA_4 interrupts a myeloperoxidase-CD11b signaling loop that perpetuates the inflammatory response, thereby redirecting PMNs to apoptosis both in vitro and in murine models of acute lung injury (49). Earlier studies also reported 15-epi-LXA_4–stimulated efferocytosis (39, 40). Our present results indicated that 15-epi-LXA_4 can effectively counter signals generated by NE, another protease released from primary granules, as it inhibited CpG DNA-evoked up-regulation of CD11b expression and NE release. One might anticipate that down-regulation of PMN CD11b expression would lead to further diminution of phagocytosis by PMNs challenged with CpG DNA. However, by preserving C5aR expression, 15-epi-LXA_4 restored phagocytosis of *E. coli* and promoted phagocytosis-induced PMN apoptosis, underscoring the importance of C5aR to antimicrobial defense. Mechanistically, augmented phagocytosis was associated with ROS-mediated increases in caspase-8 and caspase-3 activity in 15-epi-LXA_4–treated PMNs. This conclusion relies on pharmacological blockade of NADPH oxidase with DPI. Although DPI also blocks other flavoprotein-using enzymes, including NO synthase, NO is not essential for phagocytosis-induced PMN apoptosis (50). It is noteworthy that 15-epi-LXA_4 also enhanced phagocytosis of *E. coli* in blood monocytes, indicating that its actions are not exclusive to PMNs. Furthermore, 17-epi-RvD1, which binds to ALX/FPR2 (5, 31), exerted actions similar to those of 15-epi-LXA_4 on PMNs challenged with CpG DNA, suggesting that these actions are likely shared by other members of this class of proresolving mediators. Our results with pharmacological inhibitors confirm that the actions of 15-epi-LXA_4 and 17-epi-RvD1 on human PMNs were predominantly mediated via ALX/FPR2. Our data also show that these proresolving lipids effectively countered CpG DNA signals despite reduced ALX/FPR2 expression on PMNs evoked by CpG DNA and *E. coli*.

We also show that 15-epi-LXA_4 and 17-epi-RvD1 administered at near peak of inflammation facilitated *E. coli* clearance, PMN apoptosis, and efferocytosis within the lung in mice, indicating its therapeutic potential. Thus, 15-epi-LXA_4 and 17-epi-RvD1 attenuation of PMN trafficking into inflamed tissues (30–32, 34), combined with restoring phagocytosis-induced PMN apoptosis, contributes to its proresolution properties. As anticipated (5, 31, 49), 15-epi-LXA_4 reduced lung permeability and release of proinflammatory cytokines evoked by *E. coli* plus CpG DNA. The increased number of monocytes/macrophages and high percentage of monocytes/macrophages containing apoptotic bodies in the airways in response to 15-epi-LXA_4 or 17-epi-RvD1 would indicate efficient tissue repair. Phagocytosis of apoptotic PMNs and other cells by macrophages induces the release of proresolving mediators, such as IL-10 (2, 31), and likely contributes to maintaining IL-10 levels at 24 and 48 h post *E. coli*, as compared with vehicle-treated mice.

Our in vitro and in vivo results show that by restoring TLR9-mediated impaired phagocytosis, 15-epi-LXA_4 and 17-epi-RvD1 facilitate bacterial clearance by PMNs and subsequently phagocytosis-induced PMN apoptosis. These actions represent a clinically relevant mechanism for facilitating removal of emigrated PMNs despite the presence of prosurvival cues from bacteria or injured tissues, demonstrating a hitherto unrecognized mechanism for ALX/FPR2 lipid ligands to promote resolution of inflammation. These actions of 15-epi-LXA_4 and 17-epi-RvD1 resemble those of resolvin E1 and resolvin D5, which activate the leukotriene B4 receptor BLT1 (37) and receptor GPR32 (35), respectively, to regulate PMN phagocytosis, but are mediated via separate receptors and distinct molecular mechanisms.

Prior studies reported that 15-epi-LXA_4 and 17-epi-RvD1 modulate human PMN function at low to high nanomolar concentrations (30, 31, 49, 51–53). We found that high nanomolar concentrations were required to inhibit PMN responses to CpG DNA, consistent with those required to block PMN transendothelial migration (51, 52) and myeloperoxidase signaling (49). Studies on various murine inflammation models also showed that 15-epi-LXA_4 and 17-epi-RvD1 can exert beneficial actions at doses considerably lower than those used in our present study (30, 35, 51–54). Differences in experimental conditions, infectious or sterile inflammation, severity of tissue damage, local vs. systemic administration of proresolving lipids, and timing and

frequency of treatment may account for the differences observed. Similar to our study, proresolving lipids at microgram doses were reported to accelerate resolution of severe bacterial lung injury (49), polymicrobial sepsis (55), colitis (56), and ischemia-reperfusion injury in mice (57).

Considering the importance of C5aR in potentiating phagocytosis and intracellular killing of bacteria (14, 15), our findings help to explain previously reported defects in PMN function, including impaired phagocytosis and delayed apoptosis under pathological conditions, in which release of CpG DNA (19, 20) or mtDNA (18, 29) is seen. Since these conditions are often associated with increased susceptibility to secondary infections, we suggest that release of CpG DNA from proliferating bacteria represents a mechanism by which microbes may evade host defense. Mimicking by mtDNA of the actions of CpG DNA partly explains how pathologies similar to those evoked by bacteria may develop following tissue injury in the absence of infection.

In summary, our present results uncover a mechanism, involving regulation of phagocytosis and phagocytosis-induced PMN apoptosis, by which pathogen-associated CpG DNA and the danger signal mtDNA may modulate the inflammatory response, and demonstrate that restoring impaired bacterial clearance and phagocytosis-induced PMN apoptosis are important mechanisms by which aspirin-triggered 15-epi-LXA_4 and 17-epi-RvD1 facilitate resolution of acute lung inflammation. These findings also underscore ALX/FPR2 as a potential therapeutic target for combating bacterial infections.

Materials and Methods

A brief description of the materials and methods can be found below, whereas an expanded methods section can be found in *SI Appendix*.

Bacterial and Mitochondrial DNA. *E. coli* DNA (strain B; Sigma-Aldrich) was purified by extraction with phenol-chloroform and ethanol precipitation (25). Mitochondrial DNA was isolated from human neutrophils using the Mitochondrial DNA Isolation Kit (BioVision). All DNA preparations contained <5 ng of LPS per milligram DNA by *Limulus* assay.

Blood Donors. Venous blood was obtained from nonsmoking apparently healthy volunteers (male and female, 26 to 65 y old). The Clinical Research Committee at the Maisonneuve-Rosemont Hospital approved the experimental protocols (project no. 99097) and each blood donor gave written informed consent.

Neutrophil Isolation and Culture. Neutrophils (5×10^6 cells per milliliter, purity > 95%, viability > 98%, apoptotic < 2%) were resuspended in RPMI medium 1640 supplemented with 10% (vol/vol) autologous serum on a rotator with neutrophil elastase inhibitor IV (20 μM; Calbiochem), neutralizing anti-proteinase 2 Ab (5 μg/mL; Abcam), cathepsin G inhibitor (20 μM; Calbiochem), 1,10-phenantroline (4 mM; Sigma-Aldrich), and PMSF (2 mM), and then challenged with CpG DNA or mtDNA (0.4 to 1.6 μg/mL). In some experiments, PMNs were preincubated with 15-epi-LXA_4 (5S,6R,15R-trihydroxy-7E,9E,11Z,13E-eicosatetraenoic acid; 0.06 to 1 μM; Cayman Chemical) or 17-epi-RvD1 (7S,8R,17R-trihydroxy-4Z,9E,11E,13Z,15E,19Z-docosahexaenoic acid; 0.12.5 to 200 nM; Cayman Chemical) with or without the ALX/FPR2 inhibitor Boc-2 (50 μM; MP Biomedicals) or WRW4 (5 μM; Tocris) and then challenged with CpG DNA. In additional experiments, neutrophils were cultured with purified NE or PR3 (Athens Research and Technology).

CD11b, C5aR, and ALX/FPR2 Expression. PMN surface expression of CD11b, C5aR (CD88), and ALX/FPR2 was assessed using R-phycoerythrin–conjugated mouse anti-human CD11b mAb (clone D12; BD Biosciences), FITC-labeled anti-CD88 mAb (clone S5/1; BioLegend), and FITC-labeled FITC-conjugated mouse anti-human ALX/FPR2 mAb (clone 30445; R&D Systems), respectively, with flow cytometry.

Phagocytosis and Phagocytosis-Induced Cell Death. For quantitative analysis of phagocytosis, PMNs were mixed with opsonized FITC-labeled *E. coli* at a ratio of 1:7 for 30 min and intracellular fluorescence was analyzed with flow cytometry (37). To assess apoptosis following phagocytosis, PMNs were cultured for 24 h with *Saccharomyces cerevisiae* (5 yeast particles per neutrophil) or *E. coli* (7 bacteria per neutrophil) with or without 15-epi-LXA_4 (1 μM), 17-epi-RvD1 (0.2 μM), DPI (20 μM), and TLR9 inhibitory oligodeoxynucleotide 5′-tttagggttagggttaggg-3′ (1.25 or 5 μM; InvivoGen) (38) and the percentage of cells with apoptotic nuclei (condensed or fragmented chromatin) was evaluated under a fluorescence microscope (37).

Apoptosis. Apoptosis in human PMNs was assessed by annexin V staining, nuclear DNA content, mitochondrial transmembrane potential, and intracellular caspase-8 and capase-3 activity with flow cytometry (25, 37).

Proteome Profiler Arrays. Human neutrophils were challenged with CpG DNA (1.6 μg/mL) or vehicle for 30 min and lysed, and proteins were quantitated using the Human Phospho-MAPK Array Kit (R&D Systems).

Neutrophil Elastase and Proteinase 3 Release. NE and PR3 activities in conditioned culture media were analyzed by specific colorimetric enzymatic assays.

Animals. All animal experiments were performed in accordance with animal welfare guidelines and authorized by the Animal Care Committee of the Maisonneuve-Rosemont Hospital (permit nos. 2014-07 and 2015-31). The experiments were performed on female C57BL/6 mice (Charles River Laboratories) and *Tlr9*$^{-/-}$ mice (breeding pairs were obtained from Akiko Iwasaki, Yale School of Medicine, New Haven, CT).

Lung Inflammation. Lung inflammation was induced in 8- to 14-wk-old female mice by intratracheal instillation of 5×10^6 colony-forming units (CFUs) live *E. coli* (37) with or without simultaneous i.p. injection of CpG DNA (1 μg/g body weight; b.w.). At 6 h (near the peak of inflammation), mice were treated with15-epi-LXA_4 (125 ng/g b.w., i.p.) or 17-epi-RvD1 (25 ng/g b.w., i.p.), as informed from previous studies (49, 55–57).

Assessment of Inflammation. At 6, 24, or 48 h post injection of *E. coli*, lungs were lavaged or processed for analysis without lavage. BAL fluid protein and total and differential leukocyte counts were determined using standard techniques (49). Apoptosis in Ly6G-positive neutrophils was assessed by annexin V staining using flow cytometry. The percentage of macrophages containing apoptotic bodies was assessed following staining with hematoxylin and eosin (49). BAL fluid cytokine levels were measured using a multiplexed bead-based immunoassay (Bio-Plex Pro Coupled magnetic beads; Bio-Rad). BAL fluid levels of 15-epi-LXA_4 and RvD1 were assessed by selective direct ELISAs (Cayman Chemical). Lungs removed without lavage were processed for standard histological evaluation and determination of lung dry-to-wet weight ratio and tissue myeloperoxidase activity (49). Lung bacteria levels were assessed by growth on tryptic agarose using aliquots of lung homogenates.

Statistical Analysis. Results are expressed as means ± SEM. Statistical comparisons were made by ANOVA using ranks (Kruskal–Wallis test) followed by Dunn's multiple contrast hypothesis test to identify differences between various treatments or by ANOVA using ranks (Friedman test) followed by the Wilcoxon–Wilcox test for repeated measures. A value of $P < 0.05$ was considered statistically significant.

Data Availability. All data supporting the findings of this paper are available within the article and *SI Appendix*.

ACKNOWLEDGMENTS. Breeding pairs of *Tlr9*$^{-/-}$ mice were kindly provided by Prof. Akiko Iwasaki (Yale School of Medicine). We thank Julie Dubeau (Animal Care Facility, Maisonneuve-Rosemont Hospital) for maintaining our *Tlr9*$^{-/-}$ colony. This study was supported by grants from the Canadian Institutes of Health Research (MOP-97742 and MOP-102619) (to J.G.F.).

1. C. Nathan, A. Ding, Nonresolving inflammation. *Cell* **140**, 871–882 (2010).
2. D. W. Gilroy, T. Lawrence, M. Perretti, A. G. Rossi, Inflammatory resolution: New opportunities for drug discovery. *Nat. Rev. Drug Discov.* **3**, 401–416 (2004).
3. A. G. Rossi *et al.*, Cyclin-dependent kinase inhibitors enhance the resolution of inflammation by promoting inflammatory cell apoptosis. *Nat. Med.* **12**, 1056–1064 (2006).
4. R. S. Hotchkiss, I. E. Karl, The pathophysiology and treatment of sepsis. *N. Engl. J. Med.* **348**, 138–150 (2003).
5. N. Krishnamoorthy, R. E. Abdulnour, K. H. Walker, B. D. Engstrom, B. D. Levy, Specialized proresolving mediators in innate and adaptive immune responses in airway diseases. *Physiol. Rev.* **98**, 1335–1370 (2018).
6. P. M. D. Potey, A. G. Rossi, C. D. Lucas, D. A. Dorward, Neutrophils in the initiation and resolution of acute pulmonary inflammation: Understanding biological function and therapeutic potential. *J. Pathol.* **247**, 672–685 (2019).
7. W. M. Nauseef, How human neutrophils kill and degrade microbes: An integrated view. *Immunol. Rev.* **219**, 88–102 (2007).

8. S. J. Klebanoff, Myeloperoxidase: Friend and foe. *J. Leukoc. Biol.* **77**, 598–625 (2005).
9. J. B. Cowland, N. Borregaard, Granulopoiesis and granules of human neutrophils. *Immunol. Rev.* **273**, 11–28 (2016).
10. G. Döring, The role of neutrophil elastase in chronic inflammation. *Am. J. Respir. Crit. Care Med.* **150**, S114–S117 (1994).
11. D. Hartl *et al*., Cleavage of CXCR1 on neutrophils disables bacterial killing in cystic fibrosis lung disease. *Nat. Med.* **13**, 1423–1430 (2007).
12. M. Berger, R. U. Sorensen, M. F. Tosi, D. G. Dearborn, G. Döring, Complement receptor expression on neutrophils at an inflammatory site, the *Pseudomonas*-infected lung in cystic fibrosis. *J. Clin. Invest.* **84**, 1302–1313 (1989).
13. C. W. van den Berg *et al*., Mechanism of neutrophil dysfunction: Neutrophil serine proteases cleave and inactivate the C5a receptor. *J. Immunol.* **192**, 1787–1795 (2014).
14. T. E. Mollnes *et al*., Essential role of the C5a receptor in *E coli*-induced oxidative burst and phagocytosis revealed by a novel lepirudin-based human whole blood model of inflammation. *Blood* **100**, 1869–1877 (2002).
15. R. F. Guo, P. A. Ward, Role of C5a in inflammatory responses. *Annu. Rev. Immunol.* **23**, 821–852 (2005).
16. U. E. Höpken, B. Lu, N. P. Gerard, C. Gerard, The C5a chemoattractant receptor mediates mucosal defence to infection. *Nature* **383**, 86–89 (1996).
17. A. M. Krieg, CpG motifs in bacterial DNA and their immune effects. *Annu. Rev. Immunol.* **20**, 709–760 (2002).
18. A. P. West, G. S. Shadel, Mitochondrial DNA in innate immune responses and inflammatory pathology. *Nat. Rev. Immunol.* **17**, 363–375 (2017).
19. R. Ratanarat *et al*., Usefulness of a molecular strategy for the detection of bacterial DNA in patients with severe sepsis undergoing continuous renal replacement therapy. *Blood Purif.* **25**, 106–111 (2007).
20. D. A. Schwartz *et al*., CpG motifs in bacterial DNA cause inflammation in the lower respiratory tract. *J. Clin. Invest.* **100**, 68–73 (1997).
21. J. C. Deng *et al*., CpG oligodeoxynucleotides stimulate protective innate immunity against pulmonary *Klebsiella* infection. *J. Immunol.* **173**, 5148–5155 (2004).
22. P. Knuefermann *et al*., CpG oligonucleotide activates Toll-like receptor 9 and causes lung inflammation in vivo. *Respir. Res.* **8**, 72 (2007).
23. F. Hayashi, T. K. Means, A. D. Luster, Toll-like receptors stimulate human neutrophil function. *Blood* **102**, 2660–2669 (2003).
24. L. József, T. Khreiss, D. El Kebir, J. G. Filep, Activation of TLR-9 induces IL-8 secretion through peroxynitrite signaling in human neutrophils. *J. Immunol.* **176**, 1195–1202 (2006).
25. L. József, T. Khreiss, J. G. Filep, CpG motifs in bacterial DNA delay apoptosis of neutrophil granulocytes. *FASEB J.* **18**, 1776–1778 (2004).
26. S. François *et al*., Inhibition of neutrophil apoptosis by TLR agonists in whole blood: Involvement of the phosphoinositide 3-kinase/Akt and NF-kappaB signaling pathways, leading to increased levels of Mcl-1, A1, and phosphorylated Bad. *J. Immunol.* **174**, 3633–3642 (2005).
27. K. A. Krychtiuk *et al*., Mitochondrial DNA and Toll-like receptor-9 are associated with mortality in critically ill patients. *Crit. Care Med.* **43**, 2633–2641 (2015).
28. J. S. Harrington, A. M. K. Choi, K. Nakahira, Mitochondrial DNA in sepsis. *Curr. Opin. Crit. Care* **23**, 284–290 (2017).
29. Q. Zhang *et al*., Circulating mitochondrial DAMPs cause inflammatory responses to injury. *Nature* **464**, 104–107 (2010).
30. C. N. Serhan *et al*., Novel functional sets of lipid-derived mediators with antiinflammatory actions generated from omega-3 fatty acids via cyclooxygenase 2-nonsteroidal antiinflammatory drugs and transcellular processing. *J. Exp. Med.* **192**, 1197–1204 (2000).
31. C. N. Serhan, Pro-resolving lipid mediators are leads for resolution physiology. *Nature* **510**, 92–101 (2014).
32. C. N. Serhan, B. D. Levy, Resolvins in inflammation: Emergence of the pro-resolving superfamily of mediators. *J. Clin. Invest.* **128**, 2657–2669 (2018).
33. M. Perretti, F. D'Acquisto, Annexin A1 and glucocorticoids as effectors of the resolution of inflammation. *Nat. Rev. Immunol.* **9**, 62–70 (2009).
34. J. Clària, C. N. Serhan, Aspirin triggers previously undescribed bioactive eicosanoids by human endothelial cell-leukocyte interactions. *Proc. Natl. Acad. Sci. U.S.A.* **92**, 9475–9479 (1995).
35. N. Chiang *et al*., Infection regulates pro-resolving mediators that lower antibiotic requirements. *Nature* **484**, 524–528 (2012).
36. B. Zhang, J. Hirahashi, X. Cullere, T. N. Mayadas, Elucidation of molecular events leading to neutrophil apoptosis following phagocytosis: Cross-talk between caspase 8, reactive oxygen species, and MAPK/ERK activation. *J. Biol. Chem.* **278**, 28443–28454 (2003).
37. D. El Kebir, P. Gjorstrup, J. G. Filep, Resolvin E1 promotes phagocytosis-induced neutrophil apoptosis and accelerates resolution of pulmonary inflammation. *Proc. Natl. Acad. Sci. U.S.A.* **109**, 14983–14988 (2012).
38. I. Gursel *et al*., Repetitive elements in mammalian telomeres suppress bacterial DNA-induced immune activation. *J. Immunol.* **171**, 1393–1400 (2003).
39. C. Godson *et al*., Cutting edge: Lipoxins rapidly stimulate nonphlogistic phagocytosis of apoptotic neutrophils by monocyte-derived macrophages. *J. Immunol.* **164**, 1663–1667 (2000).
40. S. Mitchell *et al*., Lipoxins, aspirin-triggered epi-lipoxins, lipoxin stable analogues, and the resolution of inflammation: Stimulation of macrophage phagocytosis of apoptotic neutrophils in vivo. *J. Am. Soc. Nephrol.* **13**, 2497–2507 (2002).
41. H. Unnewehr *et al*., Changes and regulation of the C5a receptor on neutrophils during septic shock in humans. *J. Immunol.* **190**, 4215–4225 (2013).
42. S. A. Freeman *et al*., Integrins form an expanding diffusion barrier that coordinates phagocytosis. *Cell* **164**, 128–140 (2016).
43. J. D. Lambris, D. Ricklin, B. V. Geisbrecht, Complement evasion by human pathogens. *Nat. Rev. Microbiol.* **6**, 132–142 (2008).
44. S. Pandey, T. Kawai, S. Akira, Microbial sensing by Toll-like receptors and intracellular nucleic acid sensors. *Cold Spring Harb. Perspect. Biol.* **7**, a016246 (2014).
45. T. Kawai, S. Akira, The role of pattern-recognition receptors in innate immunity: Update on Toll-like receptors. *Nat. Immunol.* **11**, 373–384 (2010).
46. O. Takeuchi, S. Akira, Pattern recognition receptors and inflammation. *Cell* **140**, 805–820 (2010).
47. M. C. Maa *et al*., The iNOS/Src/FAK axis is critical in Toll-like receptor-mediated cell motility in macrophages. *Biochim. Biophys. Acta* **1813**, 136–147 (2011).
48. A. Achuthan, C. Elsegood, P. Masendycz, J. A. Hamilton, G. M. Scholz, CpG DNA enhances macrophage cell spreading by promoting the Src-family kinase-mediated phosphorylation of paxillin. *Cell. Signal.* **18**, 2252–2261 (2006).
49. D. El Kebir *et al*., 15-Epi-lipoxin A_4 inhibits myeloperoxidase signaling and enhances resolution of acute lung injury. *Am. J. Respir. Crit. Care Med.* **180**, 311–319 (2009).
50. A. Coxon *et al*., A novel role for the beta 2 integrin CD11b/CD18 in neutrophil apoptosis: A homeostatic mechanism in inflammation. *Immunity* **5**, 653–666 (1996).
51. C. N. Serhan *et al*., Resolvins: A family of bioactive products of omega-3 fatty acid transformation circuits initiated by aspirin treatment that counter proinflammation signals. *J. Exp. Med.* **196**, 1025–1037 (2002).
52. Y. P. Sun *et al*., Resolvin D1 and its aspirin-triggered 17*R* epimer. Stereochemical assignments, anti-inflammatory properties, and enzymatic inactivation. *J. Biol. Chem.* **282**, 9323–9334 (2007).
53. M. Spite *et al*., Resolvin D2 is a potent regulator of leukocytes and controls microbial sepsis. *Nature* **461**, 1287–1291 (2009).
54. R. E. Abdulnour *et al*., Aspirin-triggered resolvin D1 is produced during self-resolving gram-negative bacterial pneumonia and regulates host immune responses for the resolution of lung inflammation. *Mucosal Immunol.* **9**, 1278–1287 (2016).
55. N. Chiang, X. de la Rosa, S. Libreros, C. N. Serhan, Novel resolvin D2 receptor axis in infectious inflammation. *J. Immunol.* **198**, 842–851 (2017).
56. A. F. Bento, R. F. Claudino, R. C. Dutra, R. Marcon, J. B. Calixto, Omega-3 fatty acid-derived mediators 17(*R*)-hydroxy docosahexaenoic acid, aspirin-triggered resolvin D1 and resolvin D2 prevent experimental colitis in mice. *J. Immunol.* **187**, 1957–1969 (2011).
57. V. Brancaleone *et al*., A vasculo-protective circuit centered on lipoxin A_4 and aspirin-triggered 15-epi-lipoxin A_4 operative in murine microcirculation. *Blood* **122**, 608–617 (2013).